First-principles calculation of the structural, electronic, and magnetic properties of cubic perovskite RbXF$_3$ (X = Mn, V, Co, Fe)

Muhammad Raza ur rehman Hashmi[1,†], Muhammad Zafar[1], M Shakil[2], Atif Sattar[1], Shabbir Ahmed[1], and S A Ahmad[1]

[1] *Simulation Laboratory, Department of Physics, The Islamia University of Bahawalpur,* 63100, *Pakistan*
[2] *Department of Physics, Hafiz Hayat Campus, University of Gujrat, Gujrat, Pakistan*

(Received 19 May 2016; revised manuscript received 1 July 2016; published online 28 September 2016)

First-principles calculations by means of the full-potential linearized augmented plane wave method using the generalized gradient approximation with correlation effect correction (GGA+U) within the framework of spin polarized density functional theory (DFT+U) are used to study the structural, electronic, and magnetic properties of cubic perovskite compounds RbXF$_3$ (X = Mn, V, Co, and Fe). It is found that the calculated structural parameters, i.e., lattice constant, bulk modulus, and its pressure derivative are in good agreement with the previous results. Our results reveal that the strong spin polarization of the 3d states of the X atoms is the origin of ferromagnetism in RbXF$_3$. Cohesive energies and the magnetic moments of RbXF$_3$ have also been calculated. The calculated electronic properties show the half-metallic nature of RbCoF$_3$ and RbFeF$_3$, making these materials suitable for spintronic applications.

Keywords: fluoroperovskites, half-metallic ferromagnetism, density functional theory, electronic structures

PACS: 74.20.Pq, 71.15.Mb **DOI:** 10.1088/1674-1056/25/11/117401

1. Introduction

Half-metallic ferromagnetic materials (HFMs) have attained significant interest from both the academic as well as industrial point of view. Half-metallic ferromagnetism plays an important role in high-performance spintronic applications due to 100% spin-polarization at the Fermi level.[1,2] Therefore, it is essential to find enhanced half-metallic ferromagnetic materials with significant magnetic moments which are well suited for modern semiconductor technology. HFMs exhibit different behaviors depending upon an electron's spin directions, for instance, they act like a metal when the electrons have one spin direction and as a semiconductor/insulator for the other direction. HM materials are also used in technological applications, such as magnetic memories,[3,4] tunnel junctions,[5] magnetic devices in spintronics area,[6] and high-efficiency magnetic sensors.[7] The perovskite materials have also received a great deal of attention for their interesting characteristics like ferro-electricity,[8–10] semi-conductivity,[11] and colossal magneto resistance (CMR).[12] In fact, the HM property relates directly to the CMR phenomenon observed in numerous transition metal perovskites.[13–16] In a recent study, a perovskite compound (Ce(Fe/Cr)O$_3$) was found to be a half-metallic ferromagnet.[17] Similarly, in various other compounds, such as Ba$_2$VTO$_6$ (T = Nb and Mo),[18] ordered LaBaCo$_2$O$_6$, disordered La$_{0.5}$Ba$_{0.5}$CoO$_3$,[19] V-doped ZnSe,[20] Sr$_2$GdReO$_6$ double perovskite,[21] and PrMnO$_3$ perovskite,[22] half metallic ferro-magnetism was revealed by first-principles methods. The HFMs have special electronic structures that make them suitable to fulfil all the requirements needed for spintronic devices and magnetic sensors.

The alkali metal fluorides RbXF$_3$ (X = Mn, V, Co, and Fe) usually crystallize in the cubic ABX_3 perovskite structure (space group pm-3m). The atomic positions in RbXF$_3$ are as follows: Rb atom at (0, 0, 0), X atom at (0.5, 0.5, 0.5), and F atoms at (0, 0.5, 0.5), (0.5, 0, 0.5), (0.5, 0.5, 0). The alkali metal fluorides also have several applications in the organo-fluorine chemistry due to their fluorescent and catalytic characteristics.[23,24] In order to deeply understand the behavior of fluoroperovskite, the spintronic character and specially the magnetic properties of the RbXF$_3$ compounds are studied by the first-principles calculations. In this study, we focus on the spin effect produced by the d-states of the X elements. From the obtained results, it is noticed that the d-states of the X atoms are responsible for the magnetic interaction in these compounds. A detailed description is provided here for the structural, electronic, and magnetic properties of these compounds. The calculations are based on density functional theory (DFT) with full structural optimization using the generalized gradient approximation with strong correlation effect correction (GGA+U). The calculated results are compared with the available theoretical and experimental data. It is observed that two compounds have the ferromagnetic behavior and show the half-metallic property. To the best of our knowledge, there are not many studies about the electronic, magnetic, and half metallic studies of RbXF$_3$. The results presented in this work may provide useful vision regarding the implementation of these materials in the field of spintronics.

[†]Corresponding author. E-mail: phd.razahashmi@iub.edu.pk

© 2016 Chinese Physical Society and IOP Publishing Ltd

2. Computational details

In the present work, the structural, electronic, and magnetic properties of RbXF$_3$ are calculated by solving the Kohn–Sham equation.[25] We have carried out first-principles calculations with both full potential and linearized augmented plane-wave (FP-LAPW) methods[26] as implemented in wien2k code.[27] The charge density and the potential between the spheres are expanded in terms of crystal harmonics up to angular momenta $L = 10$. To achieve the charge and energy convergence, we expand the basis function up to $R_{\mathrm{MT}} \times K_{\mathrm{MAX}} = 8$, and the cut-off energy, which represents the separation between the core and the valance states, is set at -6.0 Ry. The number of k-points in the irreducible wedge of the Brillouin zone (BZ) are 3000. The muffin-tin (MT) radii chosen for Rb, Fe, Mn, V, Co, and F are 2.5 a.u, 1.92 a.u, 1.96 a.u, 1.94 a.u, 1.95 a.u., and 1.73 a.u., respectively. The self-consistent calculations are considered to be converged when the total energy and the charge density of the system are stable within 10^{-4} eV, and 10^{-5} eV, respectively.

The strong electron interaction effect in the X(3d) ions requires a more reliable description than that achieved by the GGA process. GGA calculations can be corrected using a strong correlation correction, also known as the GGA (LDA)+U method.[28,29] The GGA+U scheme is a useful approach for many strongly correlated systems and provides satisfactory results.[30,31] The effective parameter implemented in this study is $U_{\mathrm{eff}} = U - J$, where U and J are the Coulomb and exchange parameters, respectively. For simplicity, U is used instead of U_{eff}. The effective parameter operates on the d orbital. The near-maximum values are selected from a reasonable range of U[32] for transition metals. For instance, the U of Fe ranges from 3.0 eV to 6.0 eV, and a value of 5.0 eV is used in the calculations.

3. Results and discussion

3.1. Structural properties

We perform the structural optimization by minimizing the total charge and energy with respect to the cell parameters and the atomic positions, and obtain the equilibrium structural properties of the cubic perovskite RbXF$_3$ (X = Co, Fe, V, and Mn). The schematic diagram of the RbXF$_3$ compounds is shown in Fig. 1.

In order to calculate the ground state properties of RbXF$_3$, the total energies around the equilibrium cell volume V_{o} have been calculated. The ground state energies are determined by using Birch Murnaghan's equation of state,[33] as shown in Fig. 2. The equilibrium lattice constant (a_{o}), the bulk modulus (B), its pressure derivative (B'), and the total energy (E_{o}) of the compounds in interest are calculated and summarized in Table 1 in comparison with the previous experimental and other theoretical data. It can be observed from Table 1 that the calculated optimized lattice parameters show a slight deviation from the experimental values within 0.060 Å (−1.41%), 0.071 Å (−1.70%), 0.030 Å (−0.7%), and 0.043 Å (−1.03%) for RbMnF$_3$, RbVF$_3$, RbCoF$_3$, and MnFeF$_3$, respectively. The obtained results are in good agreement with the previous experimental results,[34] as can be seen in Fig. 3. The slight overestimation in the equilibrium lattice constant is a typical feature of GGA.[35] It can also be observed that the lattice constant a_{o} has an increasing trend along the sequence as a_{o}(RbMnF$_3$) > a_{o} (RbVF$_3$) > a_{o}(RbFeF$_3$) > a_{o}(RbCoF$_3$). The crystal rigidity can be measured by the bulk modulus

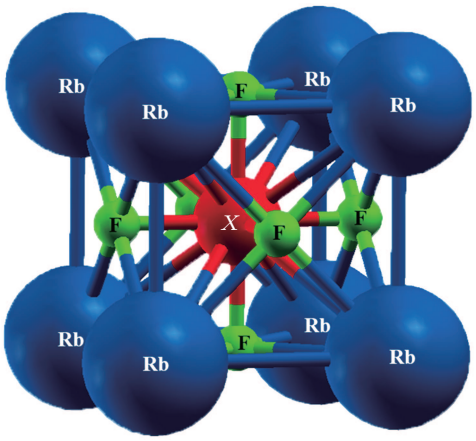


Fig. 1. (color online) Schematic diagram of RbXF$_3$ perovskite unit cell.

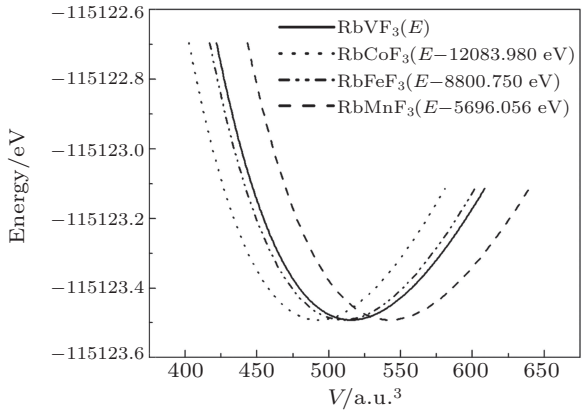


Fig. 2. The volume optimization curves for RbXF$_3$.

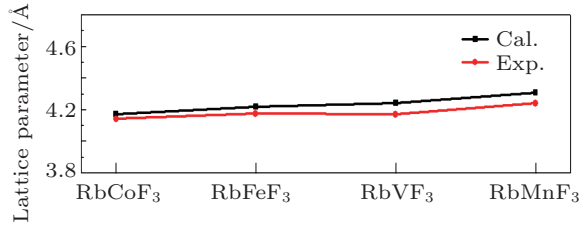


Fig. 3. (color online) Lattice constants of RbXF$_3$.

Table 1. Calculated lattice parameter a, bulk modulus B, pressure derivative B', total and cohesive energies of RbXF$_3$ (X = Mn, V, Co, Fe).

Compound		a/Å	B/GPa	B'	E_{tot}/eV	E_{Coh}/(eV/atom)
$RbMnF_3$	this work	4.3080	59.3067	4.6157	–120819.547	21.65196
	Exp.	4.24[a]				
	other theor.	4.215[a], 4.24[b] 4.252[d]	65.7[c]	–	–	
$RbVF_3$	this work	4.2437	67.01	4.8400	–115123.491	26.12812
	Exp.	4.17[a]	–	–	–	
	other theor.	4.165[a], 4.17[b] 4.203[d]	69.6[c]	–	–	
$RbCoF_3$	this work	4.1725	69.1845	4.8357	–127207.471	21.49556
	Exp.	4.141[a]	–	–	–	
	other theor.	4.108[a], 4.141[b] 4.143[d]	71.3[c]	–	–	
$RbFeF_3$	this work	4.2177	66.9202	4.8408	–123924.241	22.89306
	Exp.	4.174[a]	–	–	–	
	other theor.	4.152[a], 4.174[b] 4.191[d]	69.4[c]	–	–	

[a]Ref. [34], [b]Ref. [36], [c]Ref. [37], [d]Ref. [38].

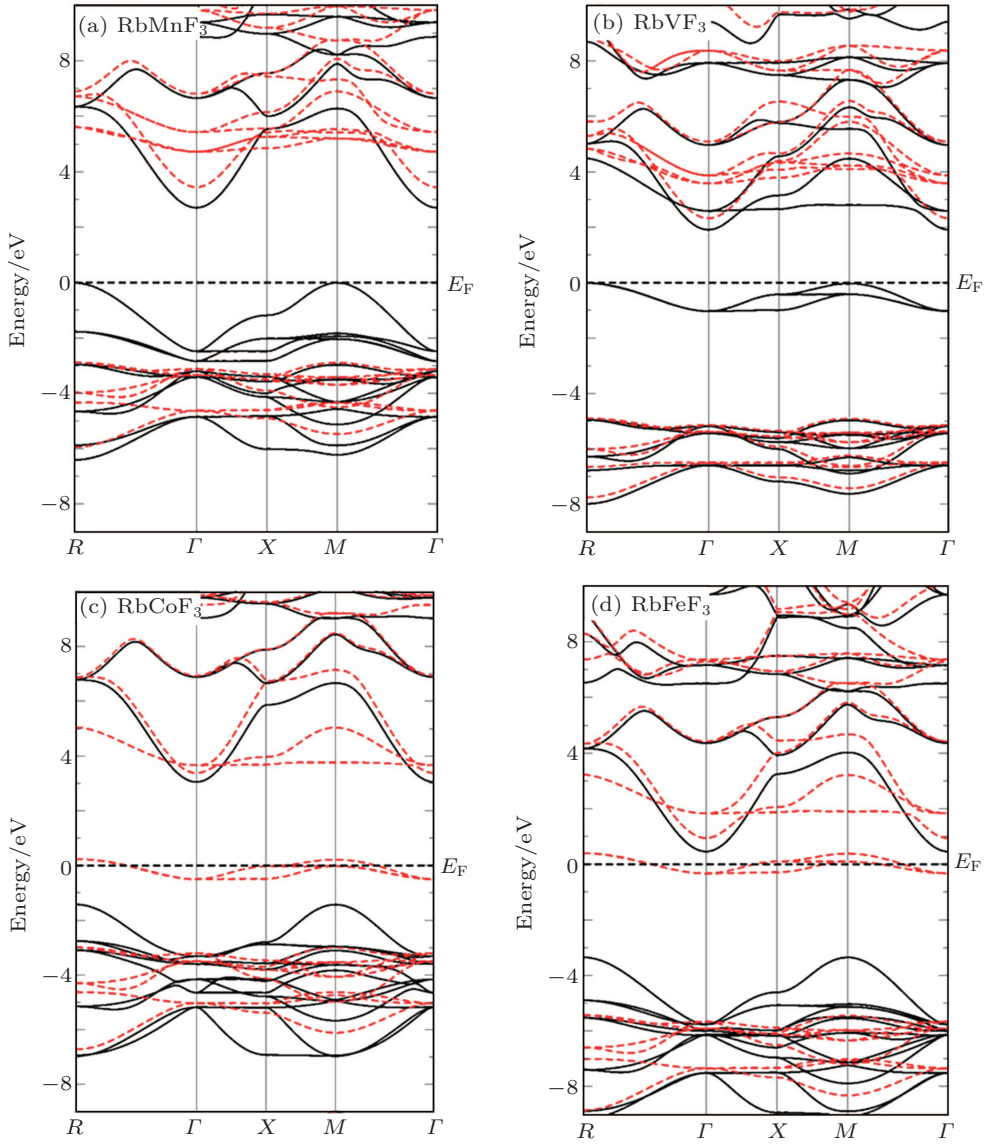


Fig. 4. (color online) The spin up (solid black) and spin down (doted red) band structures of RbXF$_3$: (a) $RbMnF_3$, (b) $RbVF_3$, (c) $RbCoF_3$, (d) $RbFeF_3$

B, so a large B represents high crystal rigidity. The bulk modulus was found to be increased in the following order: $B(\mathrm{RbCoF_3}) > B(\mathrm{RbFeF_3}) > B(\mathrm{RbVF_3}) > B(\mathrm{RbMnF_3})$. This increasing trend reveals that the compressibility as well as the hardness of the material increases in the same sequence. Our calculated bulk modulus for RbXF$_3$ also shows a reasonable agreement with that obtained by other studies as presented in Table 1.

To evaluate the bonding strength of the studied materials, the cohesive energy is calculated as

$$E_{\mathrm{Coh}} = \left(E^{\mathrm{Rb}}_{\mathrm{atom}} + E^{X}_{\mathrm{atom}} + 3E^{\mathrm{F}}_{\mathrm{atom}}\right) - E^{\mathrm{Rb}X\mathrm{F_3}}_{\mathrm{Tot}}, \qquad (1)$$

where $E^{\mathrm{Rb}X\mathrm{F_3}}_{\mathrm{Tot}}$ is the total energy of the compound at equilibrium and $E^{\mathrm{Rb}}_{\mathrm{atom}}$, E^{X}_{atom}, and $3E^{\mathrm{F}}_{\mathrm{atom}}$ are the total energies of the pure atomic components. The structural stability of $\mathrm{RbMnF_3}$, $\mathrm{RbVF_3}$, $\mathrm{RbCoF_3}$, and $\mathrm{RbFeF_3}$ is investigated by means of cohesive energy. The cohesive energy is the energy needed to decompose the compound into single atoms. Thus, the larger the calculated value, the more stable the crystal structure.[39] The obtained cohesive energies of RbXF$_3$ are presented in Table 1.

3.2. Electronic and magnetic properties

We calculate the spin-polarized band structure, the total and partial densities of states (PDOS) along the high-symmetry paths in the first Brillouin zone for the RbXF$_3$ compounds. The calculated spin-polarized band structures of the RbXF$_3$ compounds at equilibrium are presented in Fig. 4.

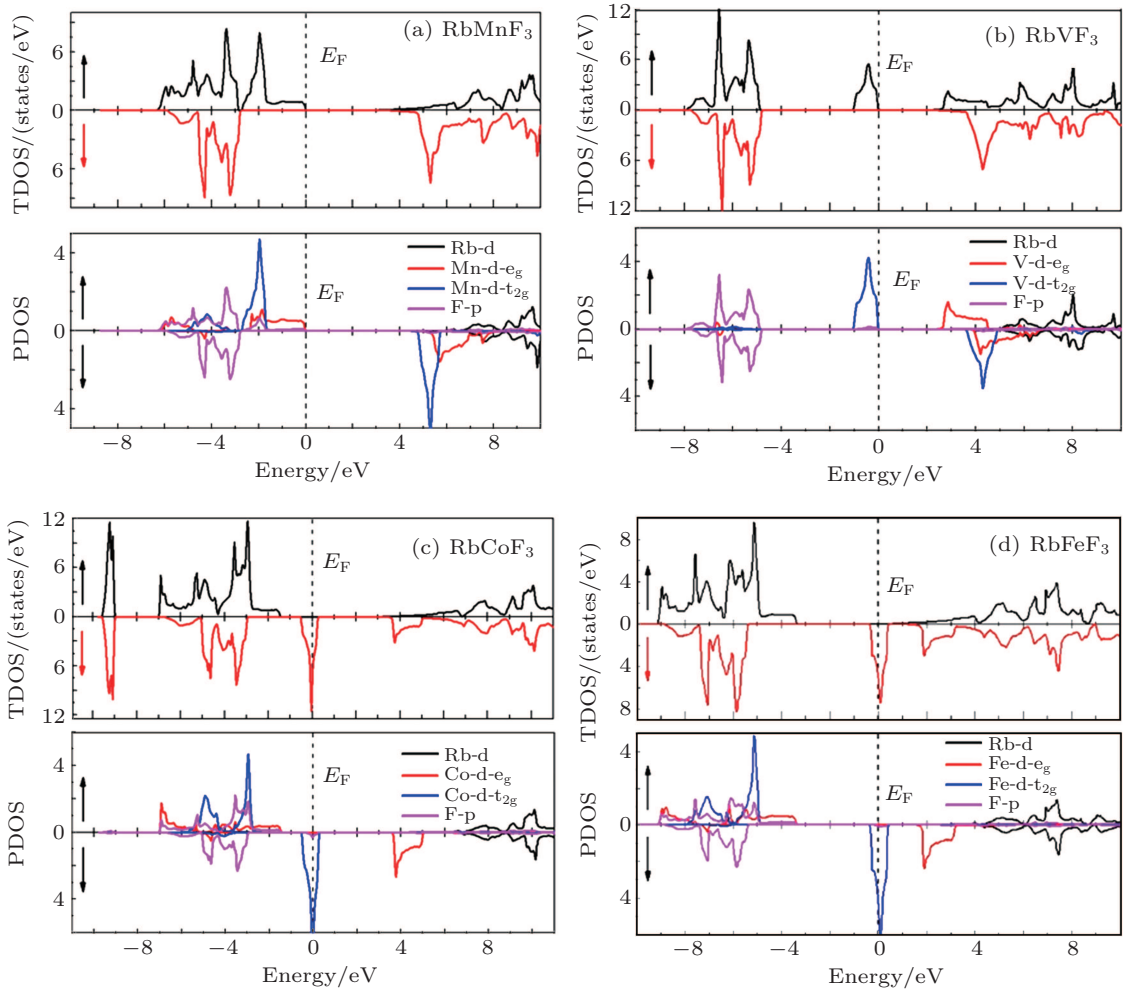


Fig. 5. (color online) The spin polarized plots for total and PDOS of RbXF$_3$: (a) $\mathrm{RbMnF_3}$, (b) $\mathrm{RbVF_3}$, (c) $\mathrm{RbCoF_3}$, (d) $\mathrm{RbFeF_3}$.

The Fermi level is set at 0 eV. It is evident that, for compounds $\mathrm{RbMnF_3}$ and $\mathrm{RbVF_3}$, the valance band maximum and the conduction band minimum are located at points R and Γ, respectively, which confirms that the material has an indirect band in nature as shown in Figs. 4(a) and 4(b). It can also be seen from Figs. 4(a) and 4(b) that the energy gaps are $E_{g\uparrow} = 2.67$ eV and $E_{g\uparrow} = 1.88$ eV for $\mathrm{RbMnF_3}$ and $\mathrm{RbVF_3}$ spin-up channels, respectively. Whereas, the energy gaps are $E_{g\downarrow} = 6.30$ eV and $E_{g\downarrow} = 7.18$ eV for $\mathrm{RbMnF_3}$ and $\mathrm{RbVF_3}$ spin-down channels, respectively. From these findings, it can be found that these compounds show semi-conducting behavior for the spin-up channel and insulating behavior for the

spin-down channel. So these compounds do not exhibit half-metallic characteristics. On the other hand, in $RbCoF_3$ and $RbFeF_3$, the energy gap is absent for the spin down channel, thus indicating their metallic behavior in the spin-down channel. While the energy gaps of $E_{g\uparrow} = 4.46$ eV and $E_{g\uparrow} = 3.74$ eV are present in the spin-up channel for $RbCoF_3$ and $RbFeF_3$, respectively, as shown in Figs. 4(c) and 4(d). From the above mentioned findings, it can be concluded that these compounds exhibit a half-metallic character.

To reveal the origin of the electronic band structure, the total and partial densities of states of these compounds are calculated and presented in Fig. 5, in which the black and red sub bands show the spin up and spin down polarizations, respectively. In case of $RbCoF_3$ and $RbFeF_3$, it is evident that in the spin down part of the total DOS, local and mostly no hybridized (Co and Fe)-d-t_{2g} states are found above the Fermi level at about 0.32 eV and 0.41 eV, respectively, which confirms their metallic behavior for the spin-down channel. Whereas the spin up channel has a band gap, resulting in 100% spin polarization of the charge carriers and making these compounds favorable in spintronics devices. It shows a half metallic behavior, with the minority of spin metallic, whereas the majority spin has insulating behavior. It can be clearly seen from Figs. 5(a) and 5(b) that $RbMnF_3$ and $RbVF_3$ compounds behave like a semi-conductor for spin up polarization and as an insulator for spin down polarization. This behavior indicates that these compounds are non-half metallic in nature.

The DOS is characterized by the strong exchange splitting of the 3d states of the X atoms, which leads to the large spin moments at their sites: $\sim 5.00\mu_B$, $\sim 2.99\mu_B$, $\sim 3.00\mu_B$, and $\sim 4.00\mu_B$ for $RbMnF_3$, $RbVF_3$, $RbCoF_3$, and $RbFeF_3$, respectively, as listed in Table 2. It can be seen that Rb and F have negligible magnetic moments, which suggests that the total magnetic moments are all contributed by the Mn/V/Co/Fe atoms. The integer value of the total magnetic moment is one significance of the half metallic nature of $RbCoF_3$ and $RbFeF_3$. Certainly, for $RbXF_3$, the spin magnetic moments are originated from the transition metal element with almost no contribution from the Rb and F sites.

Table 2. Local, interstitial, and total magnetic moments of $RbXF_3$ in units of μ_B.

Site	$RbMnF_3$	$RbVF_3$	$RbCoF_3$	$RbFeF_3$
Rb	–0.00020	0.00262	–0.00069	–0.00188
F	0.04696	0.02405	0.06643	0.06126
Mn	4.52548	–	–	–
V	–	2.41373	–	–
Co	–	–	2.74824	–
Fe	–	–	–	3.67959
Interstitial site	0.33486	0.51135	0.05338	0.13890
Total	5.00101	2.99985	3.00022	4.00039

4. Conclusion

Structural, electronic, and magnetic properties of $RbXF_3$ have been investigated by a first-principles (FP-LAPW) method. The obtained lattice constants and bulk moduli of $RbXF_3$ are in good agreement with the experimental and other theoretical data. The total DOS results within the GGA+U approach illustrate that $RbCoF_3$ and $RbFeF_3$ are half-metallic, having insulating energy-gaps in spin-up TDOS↑ and conductive behavior for spin down TDOS↓. Analysis of the electronic structure by means of PDOS for two spin orientations (PDOS↑↓) permits to infer that the $t_{2g}\downarrow$ sub-states of Co(3d) and Fe(3d) are mainly responsible for the conductive behavior of $RbCoF_3$ and $RbFeF_3$. In case of other two compounds $RbMnF_3$ and $RbVF_3$, this half metallic feature is missing. Furthermore, the total spin-magnetic moments of $RbMnF_3$, $RbVF_3$, $RbCoF_3$, and $RbFeF_3$ are $\sim 5.00\mu_B$, $\sim 2.99\mu_B$, $\sim 3.00\mu_B$, and $\sim 0.00\mu_B$, respectively.

Acknowledgment

The authors are highly obliged Dr. S A Ahmed for providing the facilities at Simulation laboratory, Department of Physics, The Islamia University of Bahawalpur, Pakistan.

References

[1] Wolf S A, Awschalom D D, Buhrman R A, Daughton J M, von Molnár S, Roukes M L, Chtchelkanova A Y and Treger D M 2001 *Science* **294** 1488
[2] Pickett W E and Moodera J S 2001 *Phys. Today* **54** 39
[3] Cheng J and Yang Z Q 2006 *Phys. Status Solidi Basic Res.* **243** 1151
[4] Sarma D D, Mahadevan P, Saha-Dasgupta T, Ray S and Kumar A 2000 *Phys. Rev. Lett.* **85** 2549
[5] Itoh H, Ohsawa T and Inoue J 2000 *Phys. Rev. Lett.* **84** 2501
[6] Bonilla C M, é Landínez Téllez D A, Arbey Rodríguez J, Vera López E and Roa-Rojas J 2007 *Physica B* **398** 208
[7] Schwarz K 1986 *J. Phys. F: Met. Phys.* **16** L211
[8] Samantaray C B, Sim H and Hwang H 2005 *Microelectronics J.* **36** 725
[9] Samantaray C B, Sim H and Hwang H 2004 *Physica B* **351** 158
[10] Bednorz J G and Muller K A 1984 *Phys. Rev. Lett.* **52** 2289
[11] Frederikse H P R, Thurber W R and Hosler W R 1964 *Phys. Rev.* **134** 442
[12] Millis A J, Shraiman B I and Mueller R 1996 *Phys. Rev. Lett.* **77** 175
[13] Kobayashi K I, Kimura T, Sawada H, Terakura K and Tokura Y 1998 *Nature* **395** 677
[14] Chan T S, Liu R S, Guo G Y, Hu S F, Lin J G, Lee J F, Jang L Y, Chang C R and Huang C Y 2004 *Solid State Commun.* **131** 531
[15] Zhang Y, Ji V and Xu K W 2012 *Physica B* **407** 2617
[16] Jeng H T and Guo G Y 2003 *Phys. Rev. B* **67** 094438
[17] Abbad A, Benstaali W, Bentounes H A, Bentata S and Benmalem Y 2016 *Solid State Commun.* **228** 36
[18] Musa Saad M 2012 *Solid State Commun.* **152** 1230
[19] Maria J, Nazir S, Alay-e-Abbas S M and Shaukat A 2014 *J. Magn. Magn. Mater.* **368** 230
[20] Monir M E A, Baltache H, Murtaza G, Khenata R, Ahmed W K, Bouhemadou A, Omran S Bin and Seddik T 2015 *J. Magn. Magn. Mater.* **374** 50
[21] Berri S 2015 *J. Magn. Magn. Mater.* **385** 124
[22] Bouadjemi B, Bentata S, Abbad A, Benstaali W and Bouhafs B 2013 *Solid State Commun.* **168** 6
[23] Sahnoun M, Zbiri M, Daul C, Khenata R, Baltache H and Driz M 2005 *Mater. Chem. Phys.* **91** 185
[24] Yakobson G G and Akhmetova N E 1983 *Synthesis* **1983** 169

[25] Kohn W and Sham L J 1965 *Phys. Rev. B* **140** 1133

[26] Andersen O K 1975 *Phys. Rev. B* **12** 3060

[27] Blaha P, Schwarz K, Madsen G K H, Kvasnicka D and Luitz J 2001 *An Augmented Plane Wave+Local Orbitals Program for Calculating Crystal Properties*

[28] Anisimov V I, Zaanen J and Andersen O K 1991 *Phys. Rev. B* **44** 943

[29] Lichtenstein A I, Anisimov V I and Zaanen J 1995 *Phys. Rev. B* **52** R5467

[30] Lichtenstein V I A 1997 *J. Phys.: Condens. Matter* **9** 767

[31] Jiang X and Guo G Y 2004 *Phys. Rev. B* **70** 035110

[32] Solovyev I V, Dederichs P H and Anisimov V I 1994 *Phys. Rev. B* **50** 16861

[33] Murnaghan F D 1944 *Proc. Natl. Acad. Sci. USA* **30** 244

[34] Moreira R L and Dias A 2007 *J. Phys. Chem. Solids* **68** 1617

[35] Jaffe J, Snyder J, Lin Z and Hess A 2000 *Phys. Rev. B* **62** 1660

[36] Ubic R 2007 *J. Am. Ceram. Soc.* **90** 3326

[37] Verma A S and Kumar A 2012 *J. Alloys Compd.* **541** 210

[38] Jiang L Q, Guo J K, Liu H B, Zhu M, Zhou X, Wu P and Li C H 2006 *J. Phys. Chem. Soli.* **67** 1531

[39] Sahu B R 1997 *Mater. Sci. Eng. B* **49** 74